Phonon activity and intermediate glassy phase of YVO_3

Néstor E. Massa*
Laboratorio Nacional de Investigación y Servicios en Espectroscopía Optica, Centro CEQUINOR, Universidad Nacional de La Plata, Casilla de Correo 962, 1900 La Plata, Argentina

Cínthia Piamonteze
Laboratório Nacional de Luz Síncrotron, Caixa Postal 6192, 13083-970, Campinas, São Paulo, Brazil and Instituto de Física, Universidade Estadual de Campinas, 13083-970, Campinas, São Paulo, Brazil

Hélio C. N. Tolentino
Laboratório Nacional de Luz Síncrotron, Caixa Postal 6192, 13083-970, Campinas, São Paulo, Brazil

José Antonio Alonso, María Jesús Martínez-Lope, and María Teresa Casais
Instituto de Ciencia de Materiales de Madrid, Consejo Superior de Investigaciones Científicas, Cantoblanco, E-28049 Madrid, Spain
(Received 8 August 2003; published 25 February 2004)

We show that in YVO_3 additional hard phonons gradually become zone center infrared active below ~210 K, verifying that a lattice phase transition takes place at about that temperature. Their gradual increment in intensity between ~210 and ~77 K is associated with a ''glassy'' behavior found in the temperature-dependent V *K* edge pseudoradial distribution. This translates into an increase in the Debye-Waller factors ascribed to the appearance of V local structural disorder below ~150 K. Conflicts between various ordering mechanisms in YVO_3 bring up similarities of the intermediate phase to known results in dielectric incommensurate systems, suggesting the formation of commensurate domains below 116 K, the onset temperature of *G*-type antiferromagnetism. We propose that ~210 and ~77 K be understood as the temperatures where the commensurate-incommensurate and incommensurate-commensurate ''lock-in'' phase transitions take place. We found support for this interpretation in the inverted λ shapes of the measured heat capacity and in the overall temperature dependence of the hard phonons.

DOI: 10.1103/PhysRevB.69.054111 PACS number(s): 64.70.Kb, 61.10.Ht, 78.30.Ly, 63.20.Ry

A plethora of oxides with perovskite structure have been described in recent decades, with fascinating electrical or magnetic properties ranging from high-T_c superconductivity to colossal magnetoresistence or ferroelectricity. Among them, the RVO_3 vanadates (R=rare earth and Y) are canted spin antiferromagnets,[1] forming a family in which anharmonicities, lattice instabilities, and Jahn-Teller distortions, intermixed with complex magnetic arrangements, are expected to play a non-negligible role in the phonon response. It is known that transition metal oxides, in general, are materials predisposed to easily contain lattice imperfections in a nominally pure phase. These imperfections, the result of competitive interactions, produce fluctuations around an average structure not matching the adjoining short-range order, i.e., there is an absence of translational symmetry in that one atomic position does not exactly repeat from cell to cell in at least one crystallographic direction, while the overall long-range lattice symmetries are maintained. We may also expect activating mechanisms depending on the coherence of those borderline fluctuating areas that, on exceeding some critical value, fuse into a lattice arrangement in which the short- and long-range order is once again preserved. Thus, understanding the orbital degrees of freedom and short-range anisotropies in confined lattice deformations will clarify the role of triggering instabilities yielding to distortions that might be responsible for a lower-symmetry phase transition.

Here we focus our attention on YVO_3, a compound regarded as a Mott-Hubbard insulator.[2] It is an orthorhombic distorted perovskite belonging at room temperature to the *Pbnm* space group, where the rare earth size favors the $GdFeO_3$ structure, a distortion that may also be incremented by contributing Jahn-Teller effects. The V^{3+} ions, at octahedral sites, show a $3d^2$ electronic configuration with spin $S=1$, where the t_{2g} orbitals, orthogonal in the cubic phase, are filled with two electrons.

The magnetic properties of YVO_3 have been exhaustively studied.[3] Multiple and reversible sign changes in the magnetization also result in a temperature interval in which the magnetic moment is oriented in a direction opposite to the applied magnetic field. The passage from a paramagnetic regime to a nearly antiferromagnetic (AFM) one below T_{N1} ~116 K is achieved by canting, yielding a *C*-type AFM structure that holds down to ~77 K.[4] Remarkably, the net magnetization in single crystals increases to a maximum and then decreases to reach negative values at about 95 K. It is claimed that spin reorientations at these temperatures are not accompanied by structural changes.[3] At temperatures close to 77 K, $\sim T_{N2}$, where the structural transition into a monoclinic distortion takes place, the net moment switches again to positive values in a *C*-type AFM that consolidates only at ~50 K.[5] It is found that the distinct magnetic orderings undergo simultaneous changes of orbital ordering and show hysteretic behavior. *G*-type orbital ordering has also been reported below 77 K by resonant x-ray scattering at the vanadium K edge.[6]

Thus, since it is known that in oxides the lattice plays a determining role in intrinsic properties, a phonon study as a function of temperature is pertinent in order to relate the

 ©2004 The American Physical Society

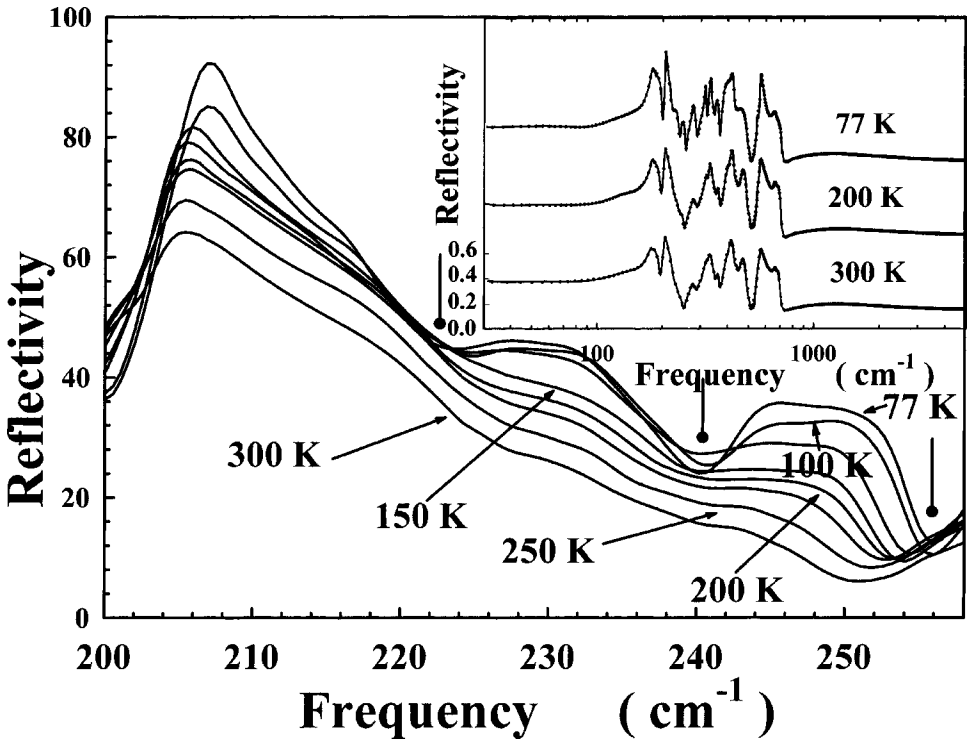

FIG. 1. Lattice phonons emerging between 200 and 77 K due to the folding of the Brillouin zone. Lines with filled circles mark longitudinal optical mode frequencies. The inset shows the reflectivity of YVO_3 at 300, 200, and 77 K. For clarity, the spectra at 200 and 77 K have been offset by an arbitrary constant.

findings to local structure deviations. This might correlate with the magnetic anomalies noted in the preceding paragraphs by relating short-range features to temperature-dependent defective orbital mixing and octahedral distortion, implying the separate formation of nanoclusters in the intermediate phase of YVO_3. Our studies are also partially motivated by the recently reported failure of first-principle calculations in describing the intermediate phase of YVO_3 as it has been described in the literature.[7]

Here, we report infrared temperature-dependent measurements of polycrystalline samples of YVO_3 (Ref. 8) and further interpret those spectra with extended x-ray absorption fine structure (EXAFS) studies of the V *K* edge.

Our temperature-dependent spectra were obtained using a Fourier transform IR Bruker 113v interferometer in the 30–10 000 cm^{-1} frequency range with samples mounted on the cold finger of an Oxford DN 1754 cryostat. The temperature stability was 0.1 K. Reflectivity measurements were made on pure polycrystalline pellets, while semitransparent CsI and polyethylene 1-cm-diam pellets, embedded randomly with YVO_3 microcrystals, were also made in order to determine the transmission spectra. They have 2 and 1 cm^{-1} resolution, respectively. For reflectivity measurements, a gold mirror was used as a 100% reference.

EXAFS measurements were recorded using the XAS beamline installed at the 1.37 GeV storage ring of the Laboratório Nacional de Luz Síncroton at Campinas, Brazil.[9] For this purpose, portions of the pure samples used in our infrared reflectivity study were reduced to fine powder in an agate mortar. The fine-ground powder, washed with alcohol, was then spread onto a nitrocellulose filter, resulting after evaporation in a uniformly thick film.

Single-phase YVO_3 samples were prepared in polycrystalline form by soft-chemistry procedures. Y_2O_3 and NH_4VO_3 were dissolved in citric acid, and the citrate solutions were dried and decomposed in air at 700 °C leading to homogeneous and reactive precursor powers. The precursors were subsequently annealed under reducing flows (H_2/N_2) at temperatures of 1100–1160 °C. We also prepared YVO_3 by solid state reactions under 20 kbar and 1000 °C. Both sets of samples yielded the same results.

Primary characterization of our samples has been done by x-ray diffraction at room temperature. In addition, neutron powder diffraction experiments were performed at the D2B high-resolution diffractometer at the Institut Laue Langevin, Grenoble. The patterns refined by the Rietveld method yielded at room temperature the conventional *Pbnm*-D_{2h}^{16} space group while at 2 K a best fit was achieved with the monoclinic P21/*n* space group with two different octahedral environments. It is important, however, to note that although overall our structural results agree with those by Blake *et al.*[10] we also share their concerns about diffraction data acquisition and analysis particularly in the 200–77 K temperature range.

The room temperature infrared reflectivity spectra of YVO_3 are identifiable with those of any other $GdFeO_3$ distorted perovskite.[11,12] At room temperature there are nine well-defined bands that correspond to lattice, antisymmetric, and symmetric stretching modes of the perovskite lattice centered at ≈200, ≈400, and ≈650 cm^{-1}, respectively (inset, Fig. 1). They may be considered as envelopes of all room

TABLE I. Fitting parameters for the reflectivity of YVO_3.

T (K)	ε_∞	Ω_{TO} (cm^{-1})	Ω_{LO} (cm^{-1})	γ_{TO} (cm^{-1})	γ_{LO} (cm^{-1})	S_j (cm^{-2})
300	2.45	90.4	102.6	546.0	493.5	3.38
		140.6	142.3	33.9	37.8	1.05
		175.0	176.8	7.5	9.5	0.4
		182.7	195.5	17.1	10.4	2.3
		203.1	218.9	4.9	60.9	0.76
		230.3	242.6	105.6	39.1	0.38
		248.7	250.0	12.8	8.4	**0.02**
		277.6	283.8	17.2	21.7	**0.32**
		320.5	325.5	18.9	14.0	0.88
		328.7	359.0	11.2	39.0	0.50
		360.2	361.4	6.6	11.4	0.002
		395.2	403.6	17.0	22.5	0.53
		408.9	447.7	12.6	50.5	0.32
		461.9	507.7	27.4	32.9	0.17
		561.8	627.1	15.0	249.0	0.27
		667.9	668.3	20.8	18.2	0.003
		677.5	702.6	61.7	32.7	0.06
200	2.42	99.1	103.6	128.4	113.6	0.98
		134.6	136.7	40.7	51.3	0.45
		179.4	186.0	7.7	20.5	2.01
		190.5	195.9	12.0	7.10	0.61
		204.6	220.7	3.41	31.6	1.10
		231.2	243.6	41.4	25.3	0.42
		247.8	250.1	9.1	7.6	**0.03**
		277.9	283.6	14.7	22.5	**0.29**
		318.8	324.4	11.6	9.8	0.82
		328.7	353.4	6.4	39.1	0.53
		360.4	364.3	9.2	13.4	0.05
		395.7	412.5	15.2	21.3	0.91
		413.1	446.8	9.6	55.8	0.03
		461.3	505.5	25.1	38.3	0.20
		559.3	629.6	23.5	25.4	0.29
		657.3	659.6	23.5	25.4	0.006
		686.5	706.9	73.3	24.1	0.05
		979.9	1014.4	1283.2	2238.1	0.12
100	2.37	89.0	91.9	82.9	55.5	0.89
		156.8	169.9	232.8	22.4	3.52
		179.7	181.1	7.42	549.6	1.03
		181.7	199.8	29.7	5.2	0.45
		205.4	219.3	0.8	17.7	0.27
		231.0	237.4	18.5	8.8	0.21
		247.8	254.6	14.5	6.0	**0.18**
		276.1	285.4	13.6	18.2	**0.31**
		315.3	323.5	10.3	15.2	0.44
		330.2	340.1	4.00	20.1	0.19
		357.2	365.8	14.6	10.2	0.23
		388.5	416.3	21.6	65.3	0.58
		417.4	427.4	15.1	17.4	0.01
		453.8	501.9	40.4	32.5	0.29
		562.8	609.8	8.2	110.3	0.24
		646.8	674.3	53.5	70.7	0.07
		695.4	705.4	44.1	18.8	0.01
		1027.0	1038.4	1417.1	2318.1	0.04

TABLE I. (*Continued*.)

T (K)	ε_∞	Ω_{TO} (cm^{-1})	Ω_{LO} (cm^{-1})	γ_{TO} (cm^{-1})	γ_{LO} (cm^{-1})	S_j (cm^{-2})
77	2.40	89.0	91.9	93.6	61.7	0.91
		151.8	169.9	276.5	23.9	3.69
		178.8	181.9	6.05	667.5	1.13
		181.7	199.6	26.4	5.7	0.32
		205.5	217.3	0.24	16.4	0.27
		230.6	237.0	21.6	8.2	0.24
		247.4	255.2	14.5	6.7	**0.23**
		276.5	286.4	10.2	11.7	**0.34**
		313.6	320.3	5.2	7.9	0.37
		329.9	341.0	4.4	15.3	0.32
		355.4	365.7	15.5	8.3	0.28
		383.2	416.3	15.8	88.5	0.53
		417.4	425.9	24.7	19.3	0.008
		448.9	505.6	66.9	30.1	0.26
		553.1	559.9	14.3	25.5	0.07
		565.5	589.4	6.2	141.6	0.05
		654.5	669.3	55.1	47.4	0.07
		689.1	709.5	58.4	29.9	0.04
		1015.9	1025.72	1290.2	2036.1	0.03

temperature infrared allowed modes and are easily followed down to 77 K. In addition, weak phonon modes with onset at $\approx$210 K signal, as a substructure, a lattice phase transition. The most prominent hard phonons gradually emerging from a typical lattice band shoulder are shown in Fig. 1. The lattice instability, although weak, is gradually enhanced as the temperature is lowered toward 77 K through $T_{N1} \approx 116$ K, the temperature of the reported *C*-type antiferromagnetic ordering, and it is associated with weak reflections violating the *Pbnm* symmetry reported by Blake *et al.* on cooling at about 200 K.[10]

We estimated phonon frequencies (Table I) using a standard multioscillator dielectric simulation fit to our reflectivity spectra.[11] We analyzed the reflectivity spectra for each temperature, simulating infrared active features with damped Lorentzian oscillators in a classical formulation of the dielectric function. The expression for the dielectric function is given by

$$\varepsilon(\omega) = \varepsilon_\infty \prod_j \left[\frac{\omega_{jLO}^2 - \omega^2 + i\gamma_{jLO}\omega}{\omega_{jTO}^2 - \omega^2 + i\gamma_{jTO}\omega} \right], \quad (1)$$

where ε_∞ is the high-frequency dielectric function; ω_{jLO} and ω_{jTO} are the longitudinal and transverse jth optical frequencies with damping constants γ_{jLO} and γ_{jTO}, respectively.

We also calculated the jth oscillator strength S_j as

$$S_j = \omega_{jTO}^{-2} \frac{\prod_k (\omega_{kLO}^2 - \omega_{jTO}^2)}{\prod_{k \neq j} (\omega_{kTO}^2 - \omega_{jTO}^2)}. \quad (2)$$

The extra zone center optical activity observed here means a net Brillouin zone folding between 210 and 77 K. Consequently, in agreement with conclusions by Ren *et al.*,[3] we do not observe additional infrared active modes, as the lower lattice symmetry is already present above T_{N1}, changing continuously through it. The dielectric simulation analysis yields phonon strengths (those in bold letters in Table I are plotted in Fig. 2) that allows identifying by optical means the temperature at which that phase transition takes place. Phonon intensity bands below $\sim$210 K seem to obey a very weak power law.

The main phonon lattice band at $\sim$160 cm^{-1} may be visualized as originating from Y ions moving against the VO_6 octahedra, and thus its behavior is likely related to the anomalous coordinate temperature dependence reported while orbital ordering takes place as the sample cools down through $\sim$210 K. This is the temperature for Jahn-Teller distortion onset, with two arrangements of alternating long and short V-O bonds forming two layers.[9]

In addition, that phonon activity is also mirrored by some internal mode band changes at higher frequencies, which, although they are not as well infrared resolved, reflect octahedral distortion in the intermediate phase.

The vibrational and structural findings are also supported by temperature-dependent EXAFS results. Figure 3 shows the Fourier transform (FT) amplitude of the EXAFS signal measured around the V *K* edge, which represents the pseudo–radial distribution function around the V atoms. It is important to remark that the *R* axis does not correspond to the atomic separation, because a phase shift correction, intrinsic to the EXAFS analysis, was not yet taken into account. If there is no structural modification, the expected behavior for the FT curves is decreasing amplitude as temperature increases due to thermal damping. This monotonic decrease is seen, for instance, for metal-to-metal bonding (V-V). Considering the first peak of the FT curves, which

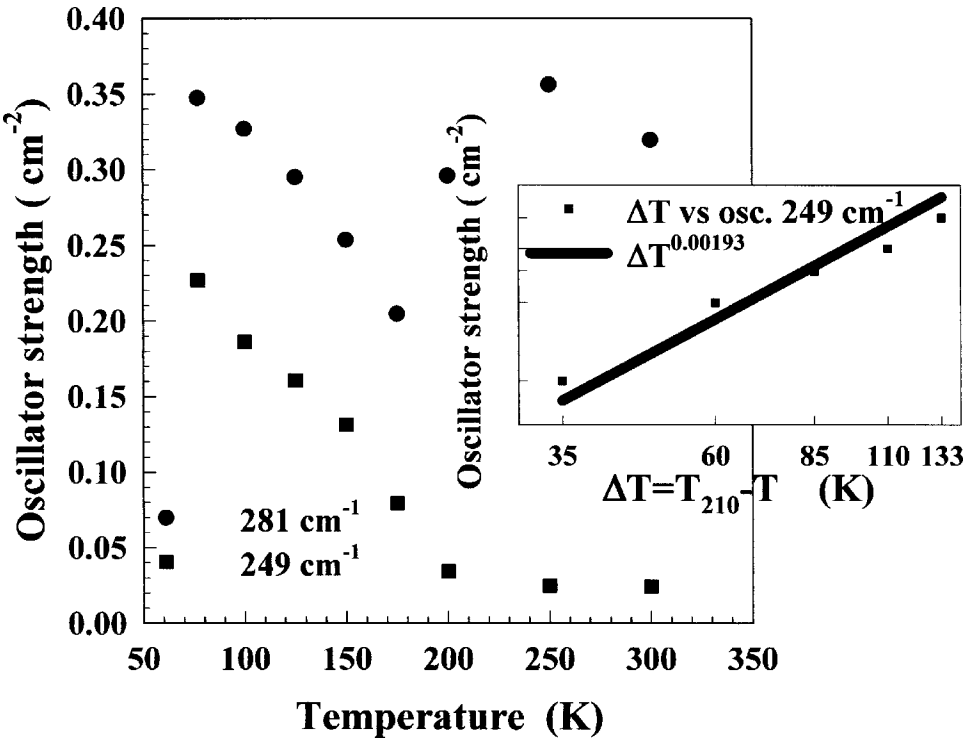

FIG. 2. Phonon oscillator strengths in the intermediate phase of YVO_3.

corresponds to the V-O neighbor shell, anomalous behavior is seen for the data measured below 150 K. In order to quantify the amplitude variation as a function of temperature, the V-O peak was analyzed considering three fixed V-O bond distances (inset, Fig. 4) using as a model starting place the parameters previously found by Blake *et al.*[10] from neutron diffraction measurements. The Debye-Waller factor was maintained the same for the three distances and, therefore, it represents the disorder averaged over all directions relative to the model. The relative Debye-Waller factor ($\Delta\sigma^2$) obtained from this analysis[13] plotted against temperature (Fig. 4) shows a monotonic decrease with temperature down to 100 K. Below 150 K an increase in σ^2 is clearly observed, with a maximum at about 50 K, the onset of AFM ordering in the low-temperature monoclinic phase.[5] Since the Debye-Waller factor measured by EXAFS takes into account both thermal and structural disorder, this increase (Fig. 4) is ascribed to the appearance of V local structural disorder.

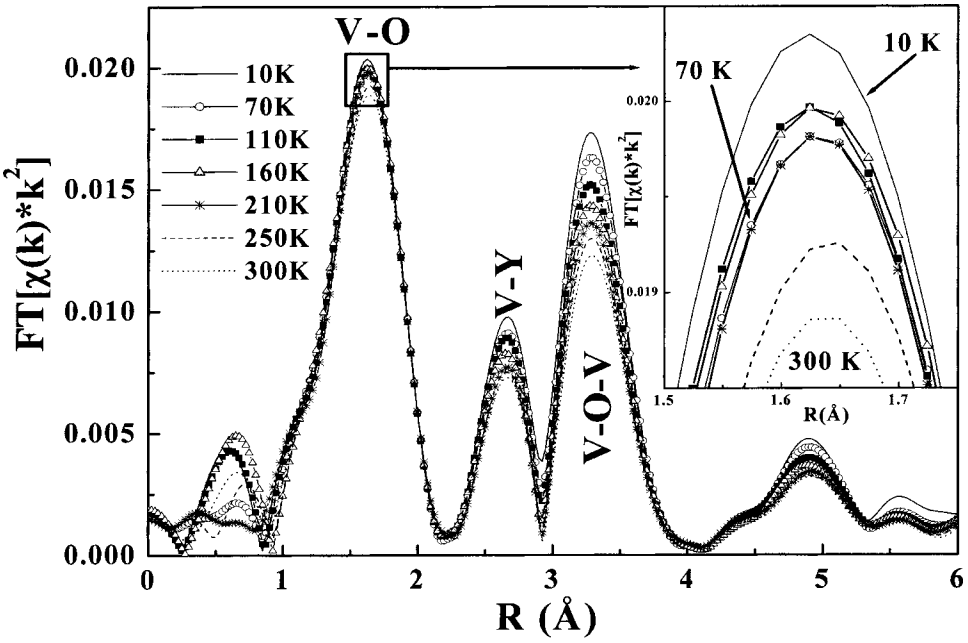

FIG. 3. Fourier transform of EXAFS signal representing the pseudoradial distribution function around V atoms. Inset: Detail of the pseudoradial distribution function for V nearest neighbors.

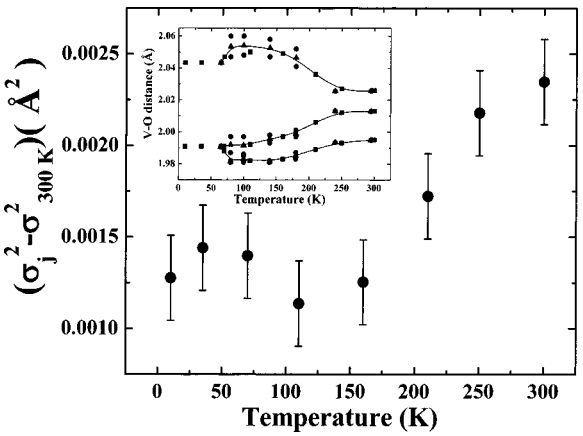

FIG. 4. Temperature dependence of the mean relative Debye-Waller factor obtained from a fitting using three different fixed V-O distances. The inset explains the model used in the fit. The stars show the distances found by neutron diffraction measurements after Ref. 10. The open triangles are the average distances indicated by EXAFS and, finally, the filled squares are the distances used in the fit for the temperatures of the EXAFS measurements. The full line is a guide for the eye.

In a perovskite lattice with transition metal ions there are two competing Jahn-Teller (JT) distortions, of *a* and *d* type, with elongation or shortening within the basal plane. They differ only in the way they are stacked.[14] We may understand the above scenario and the gradual increment in phonon intensity as due to a progressively more pronounced $GdFeO_3$ distortion driven by the octahedra tilting and rotation. As Mizokawa *et al.*[15] point out, at ~210 K, cooling toward 116 K, the system starts with energies of a *C*-type AFM, compatible with an *a*-type JT distortion, almost degenerate with that for a *G*-type AFM *d* type JT distortion, and thus the net lattice distortion is nearly suppressed at these higher temperatures. Below 116 K, the *C*-type antiferromagnetism favors an *a*-type JT distortion taking hold and, since a more pronounced lower-temperature $GdFeO_3$ tilting favors the *G*-type AFM state, the onset of a distorted *G*-type AFM consolidates at 77 K, the temperature of the first-order structural phase transition.

Further, as was somewhat anticipated above, we note that from the lattice point of view these competitive interactions, conflicts between various ordering mechanisms resulting from faulty orbital arrangements, imply instabilities that in our case will also likely be related to the Jahn-Teller distortion in the *ab* plane below 210 K. This competition causes frustration and intergrowth, yielding an incommensurate ion arrangement, i.e., long-range order but no translational symmetry, since an atomic position is not exactly repeated from cell to cell in at least one crystallographic direction.[16] In YVO_3, although superlattice reflections have not been detected in the temperature interval from 210 to 77 K, this situation is found in orbital mismatching of the *ab* plane. This is supported by the infrared active hard phonons discussed here resembling the overall behavior already found in incommensurate prototype materials such as K_2SeO_4.[17] By now it is accepted that in oxides nanoscale phase separation appearing as intrinsic lattice inhomogenieties is a feature revealing a phenomenology similar to that of manganese oxides, which may even be extended to cuprates.[18] YVO_3, being an insulator in the whole temperature range, provides an unusual and comprehensible window to look at this phenomenon. Having faulty orbital ordering in the *ab* plane immediately below ~210 K, the above perspective yields an average crystal symmetry close or equal to that of the higher-temperature phase and, on cooling toward 77 K, we would expect the appearance of domains that carry inside them the essence of the low-temperature ordered phase. This cluster nucleation and growth would trigger the broad first-order transition ''locking in'' the lattice periodicity at ~77 K and it would explain the origin of short-range orbital fluctuations that, being weak, do not alter the overall long-range ordering at a length scale of 1000 Å.[10] This proposition also helps to solve the riddle found in first-principles calculations needing persistence of the low-temperature phase distortion in the intermediate phase, requiring more than 50% of it.[7] We also add that around 77 K microdislocation mechanisms can cause the hysteretic behavior found.[10]

The magnetic order onset at ~116 K might be identified with a change in lattice regime from orthorhombiclike to more monocliniclike, and magnetic reversal would be related to the orbital quasiorder altering the canting angle locally, signaling to a more sensitive magnetic probe the onset of cluster formation in a soliton regime. As in the case of incommensurate dielectrics we did not expect to detect nor did we observe that change of regime by optical means.[19]

On the other hand, it is worth mentioning that specific heat measurements by Borukhovich *et al.*[20] and, more recently, by Blake *et al.*[10] show transitions having characteristic inverted λ shapes with a long tail on the low-temperature side extending all the way to 77 K and beyond. In addition to a magnetic role in YVO_3, lattice contributions yield very broad transitions that are similar to what has been found for incommensurate phases in prototype A_2BX_4 systems.[21,22] The inverted λ shape is consistent with discommensuration, here related to a non-negligible orbital disorder, and it is opposite to the behavior found at structural and other phase transitions. We note that it has been established that in incommensurate dielectrics the normal-incommensurate transition the enthalpy and entropy are generally much larger than

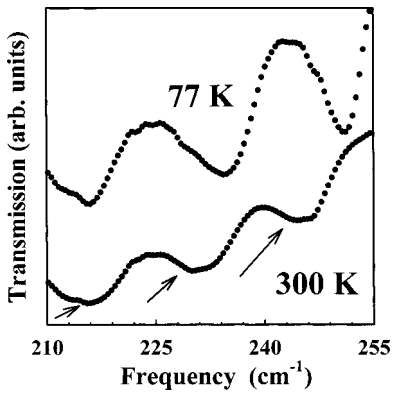

FIG. 5. Transmission spectra of lattice phonon sidebands in 1 cm^{-1} resolution spectra of YVO_3 between 225 and 210 cm^{-1} at 300 and 77 K.

those of incommensurate-commensurate transitions. On the high-temperature side the heat capacity decreases rapidly.[21]

Finally, another point to remark is that YVO_3 is inherently highly anharmonic even at room temperature. Figure 5 shows 1 cm^{-1} resolution infrared transmission measurements with defined very weak substructures in a phonon lattice band related to the sharper structure, shown in Fig. 1 in the reflectivity, for the same frequency range. This indicates that lattice inhomogeneities are also present at room temperature within a local mode picture, thus passing undetected by techniques dealing with long-range ordering and Rietveld analyses. In essence, they reveal a latent symmetry that is lower than orthorhombic *Pbmn*-D_{2h}^{16} even at 300 K at some spots of the YVO_3 lattice. On the other hand, it is then significant to note that resonant x-ray diffraction studies suggest that the *G*-type orbital ordering starts at room temperature.[23]

Summarizing, we have shown that hard phonons become infrared active below 210 K. We propose that the gradual net Brillouin zone center folding may originate from faulty orbital stacking due to local energetically prevailing distortions between ~210 and ~77 K. Fluctuations around an average structure may be the consequence, as in dielectrics, of lattice regions that do not match the higher-temperature order and that, on cooling toward T_{N2}, will experience activating mechanisms involving growth in the coherence of borderline fluctuating areas which, exceeding some critical value, would trigger the low-temperature monoclinic ordered phase. We associated this with the observed anomalous Debye-Waller factors which show an increase between ~150 and ~70 K attributed to V local structural disorder. It is thus proposed that ~210 and ~77 K be assigned as the temperatures for possible commensurate-incommensurate and incommensurate-commensurate ''lock-in'' lattice phase transitions, respectively. We conclude that the intermediate phase of YVO_3 provides a rich ground of interactions that remain to be explored.

N.E.M. acknowledges an enlightening exchange of e-mails with T. T. M. Palstra (University of Groningen, Netherlands). J.A.A., M.J.M-L., and M.T.C. acknowledge the financial assistance of the Ministerio de Ciencia y Tecnología under Project No. MAT2001-0539. C.P. also acknowledges a Ph.D. grant (Grant No. PROC. 00/00789-3) from the funding agency of the state of São Paulo (FAPESP), Brazil, and the Laboratorio Nacional de Investigación y Servicios en Espectroscopía Optica thanks the CLAF (Centro LatinoAmericano de Física) for an emergency maintenance grant.

*Email address: nem@dalton.quimica.unlp.edu.ar

[1] H. C. Nguyen and J. B. Goodenough, Phys. Rev. B **52**, 324 (1995).

[2] H. F. Pen, M. Abbate, A. Fujimori, Y. Tokura, H. Esaki, S. Uchida, and G. A. Sawatzky, Phys. Rev. B **59**, 7422 (1999).

[3] Y. Ren, T. T. M. Palstra, D. I. Khomskii, A. A. Nugroho, A. A. Menovsky, and G. A. Sawastzky, Phys. Rev. B **62**, 6577 (2000), and references therein.

[4] *C*-type magnetic ordering (*G*-type orbital ordering) is antiferromagnetic in the *ab* plane and ferromagnetic in the *c* direction.

[5] *G*-type magnetic ordering (*C*-type orbital ordering) implies antiferromagnetism in all crystallographic directions.

[6] M. Noguchi, A. Nakazawa, T. Arima, Y. Wakabayashi, H. Nakao, and Y. Murakami, Phys. Rev. B **62**, R9271 (2000).

[7] Z. Fang, N. Nagaosa, and K. Terakura, Phys. Rev. B **67**, 035101 (2003).

[8] Preliminary results were presented at the Fifth Latin American Workshop on Magnetism, Magnetic Materials and their Applications, Bariloche, Argentina, 2001.

[9] H. Tolentino, J. C. Cezar, D. Z. Cruz, V. Compagnon-Cailhol, E. Tamura, and M. C. M. Alves, J. Synchrotron Radiat. **5**, 521 (1998).

[10] G. B. Blake, T. T. M. Palstra, Y. Ren, A. A. Nugrobo, and A. A. Menovsky, Phys. Rev. Lett. **87**, 245501 (2001); G. R. Blake, T. T. M. Palstra, Y. Ren, A. A. Nugroho, and A. A. Menovsky, Phys. Rev. B **65**, 174112 (2002).

[11] N. E. Massa, H. Falcon, H. Salva, and R. E. Carbonio, Phys. Rev. B **56**, 10 178 (1997).

[12] M. Couzi and P. V. Huong, J. Chim. Phys.-Chim. Biol. **69**, 1339 (1972).

[13] There is an YVO_3 room temperature spectrum reported in the earlier literature [M. Kasuya, Y. Tokura, T. Arima, H. Eisaki, and S. Uchida, Phys. Rev. B **47**, 6197 (1993)] that agrees with our profile. Our sharper features are likely due to a higher-resolution recording.

[14] Bruce Ravel, *EXAFS Analysis Using FEFF and FEFFIT*, Department of Physics, FM-15, University of Washington, Seattle, WA 98195, U.S.A. http://fe_.phys.washington.edu/~ravel/

[15] We thank T. T. M. Palstra for clarifying this point. See also J. B. Goodenough, Phys. Rev. **150**, 564 (1955); **171**, 466 (1968).

[16] T. Mizokawa, D. I. Khomskii, and G. A. Sawatzky, Phys. Rev. B **60**, 7309 (1999).

[17] J. D. Axe, M. Iizumi, and G. Shirane, in *Incommensurate Phases in Dielectrics*, edited by R. Blinc and A. P. Levanyuk (Elsevier, Amsterdam, 1986).

[18] E. Dagotto, J. Burgy, and A. Moreo, Solid State Commun. **126**, 9 (2003), and references therein. See also X. Qiu, S. J. L. Billinge, C. R. Kmety, and J. F. Michell, cond-mat/0307652 (unpublished).

[19] See, for example, P. Echegut, F. Gervais, and N. E. Massa, Phys. Rev. B **34**, 278 (1986), Fig. 4.

[20] A. S. Borukhovich, G. V. Bazuev, and G. P. Shweikin, Fiz. Tverd. Tela (Leningrad) **116**, 286 (1974) [Sov. Phys. Solid State **16**, 191 (1974)].

[21] R. Blinc, P. Prelovsek, V. Rutar, J. Seligar, and S. Zumer, in *Incommensurate Phases in Dielectrics* (Ref. 17), Vol. 14.1, p. 249, and references therein.

[22] Y. Ishibachi, in *Incommensurate Phases in Dielectrics* (Ref. 17), Vol. 14.2, p. 49, and references therein.

[23] M. Noguchi, A. Nakazawa, S. Oka, T. Arima, Y. Wakabayashi, H. Nakao, and Y. Murakami, Phys. Rev. B **62**, R9271 (2000).